

S. DYMEK* M. WRÓBEL*, M. Blicharski*

EFFECT OF ALLOY ADDITIONS ON PROCESSING OF TiAl-5%X (X=Cr, V, W) INTERMETALLICS BY MECHANICAL ALLOYING

WPLYW 5% AT. DODATKU Cr, V I W NA PRZEBIEG MECHANICZNEJ SYNTEZY STOPÓW NA OSNOWIE γ -TiAl

Alloys with chemical compositions TiAl48, TiAl45Cr5, TiAl45V5 and TiAl45W5 were synthesized by mechanical alloying in a Szegvari-type attritor from elemental powders of high purity. The presence of a third element (V, Cr, W) influenced the mechanical alloying process of γ -TiAl alloys. The prolong milling (100 h) of TiAl45V5 alloy led to its complete amorphisation; the milling of the TiAl45Cr5 alloy in the same conditions led also to its amorphisation but Cr(Ti, Al) solid solution was also present. Tungsten, on the other hand, did not form solid solutions. Instead, it underwent heavy refinement during milling and as a consequence, constitute a dispersoid in the consolidated material. It was shown that amorphisation of powders is preceded by formation of nanocrystalline structure in the milled powder particles in early stages of milling (6 h).

Keywords: mechanical alloying, titanium aluminides

W pracy wytworzono i badano stopy o następujących składach chemicznych: TiAl48, TiAl45Cr5, TiAl45V5 oraz TiAl45W5 (% at.). Mechaniczną syntezę tych stopów przeprowadzono w laboratoryjnym atritorze typu Szegvari z udziałem proszków czystych metali. Stwierdzono, że obecność dodatku stopowego (Cr, V, W) znacząco wpływa na przebieg procesu mechanicznego wytwarzania stopów. Długotrwałe mielenie (100 godz.) doprowadziło do całkowitej amorfizacji stopu TiAl45V5; mielenie proszków stopu TiAl45Cr5 w tych samych warunkach również prowadziło do amorfizacji, a ponadto do utworzenia roztworu stałego na osnowie Cr. Wolfram nie tworzył roztworów stałych, lecz ulegał silnemu rozdrobnieniu i w konsekwencji w materiale litym występował w postaci dyspersoidu. Wykazano, że amorfizacja proszków była poprzedzona utworzeniem struktury nanokrystalicznej w cząstkach proszków już w początkowym stadium mielenia (6 godz.).

1. Introduction

TiAl based alloys are interesting materials for high temperature applications in industrial and aviation gas turbines as well as aerospace and automobile industries. Their applicative properties include low density, high melting point, good oxidation and burn resistance as well as high yield strength and an elastic modulus which is retained at elevated temperatures [1, 2]. Nevertheless, extensive research has shown that TiAl based intermetallic materials are brittle at room temperature and quickly loose their good mechanical properties at temperatures above 700°C thus limiting their application [3, 4].

Different approaches have been attempted to improve properties of TiAl-based alloys. For example, modification of the chemical composition by alloying with substitutional elements (e.g. V, Cr, Nb, W, Mn and Si) in-

creases ductility and fracture toughness [5]. Thermomechanical treatments applied to control the size and distribution of the different phases present in Ti-Al alloys are another alternative for increasing the room temperature ductility, e.g. refinement of the lamellar microstructure [6]. An increase of ductility could also be achieved by reducing the grain size [7].

This research was aimed at the processing of TiAl-based materials modified by an addition of minor amounts of Cr, V and W. Mechanical alloying (MA) was selected as a processing route. MA offers the advantages of refining the grain sizes even to the nanoscale and the generation of non-equilibrium and amorphous phases. Also, the controlled oxygen level in milling chamber produces oxide dispersoid which is believed to contribute to the improvement of creep properties despite fine-grained microstructure.

* AGH UNIVERSITY OF SCIENCE AND TECHNOLOGY, FACULTY OF METALS ENGINEERING AND INDUSTRIAL COMPUTER SCIENCE AL. MICKIEWICZA 30, 30-059 KRAKÓW, POLAND

2. Material and experimental procedure

The alloys with the following compositions (in at.%) were synthesized: TiAl45Cr5, TiAl45V5, TiAl45W5 and TiAl48 as a referenced material. The excess of titanium with respect to stoichiometry in all alloys was aimed to assure that the alloys will exhibit two-phase microstructure. The alloys were prepared by mechanical milling of high purity elemental powders (Ti: 99.0 wt. %, Al: 99.5 wt. %, V: 99.5 wt. %, Cr: 99.95 wt.%, W:99.9 wt.%). All powders except W had average diameter less than $44\ \mu\text{m}$ (-325 mesh). The W powder size was less than $149\ \mu\text{m}$ (-100 mesh). An additional blend of the TiAl45W5 alloy was prepared from prealloyed commercial TiAl (-325 mesh) powder (Ti to Al weight ratio 64:36). All powders were purchased from Alfa Aesar Company.

Mechanical alloying was carried out in a Szegvari laboratory attritor mill in an argon atmosphere with the controlled oxygen level reduced to about 3-5 ppm. The slight positive pressure (about 20 kPa) was maintained inside the mill in order to prevent entering of air into the mill during the milling process. The milling was carried out in a $1400\ \text{cm}^3$ sealed stainless steel tank with a 3.63 kg (8 lb) charge of 4.76 mm (3/16") stainless steel balls and about 11:1 ball to powder ratio (by weight). The first stage of milling (2 to 5 h) was carried out at cryogenic temperatures, using liquid nitrogen as the coolant. The liquid nitrogen prevent relatively ductile powder particles from agglomeration on the tank walls, shaft arms and balls and also promote the initial cold fracture. The powder was sampled periodically during the milling allowing for characterization of the powder morphology and the progress of mechanical alloying process.

The changes in particle morphology during milling were examined by scanning electron microscopy (SEM). SEM was also used for examination of pre-polished powder particles sections by analyzing images formed by backscattered electrons (BSE). The X-ray phase analysis was performed with $\text{CoK}\alpha$ radiation. The X-ray diffractograms (XRD) were used for evaluation of lattice parameters, lattice strains and X-ray crystallite size. The microstructure of individual powder particles was examined by transmission electron microscopy (TEM). For this purpose, powder particles were embedded in an epoxy glue and sliced onto small pieces on a Reichert microtome.

A sample of as-milled powder of each alloy was also annealed at 1000°C for 5 h. The annealed powders were subjected to XRD analysis.

3. Results and discussion

Powders

The mechanical milling process of all alloys but that one with tungsten proceeded in a similar manner. The

change in particle size and morphology during mechanical alloying process was typical for milling of ductile powders [8]. Initially, the increase in particle size and their flattening was observed. This was due to the predominance of welding over fracturing occurring in the relatively soft particles. Many of them approached size about $500\ \mu\text{m}$, however, a significant scatter in particle size was observed. The shape of particles changed to more spheroidal with milling time. After 50 h of milling particles became much finer indicating predominance of fracturing over welding but the rough particle surface showed that welding was still in work. The 100 h of milling produced uniform powder with almost spherical particles with smooth surfaces. Fig. 1 shows the powder particle morphology of TiAl5X alloy after 100 h of milling. The average size of powder particle (after sieving through a $45\ \mu\text{m}$ mesh) was about $10\ \mu\text{m}$. Both point and map EDS analyses showed that the chemical composition of individual particles was uniform and corresponded to the starting composition of a particular powder blend.

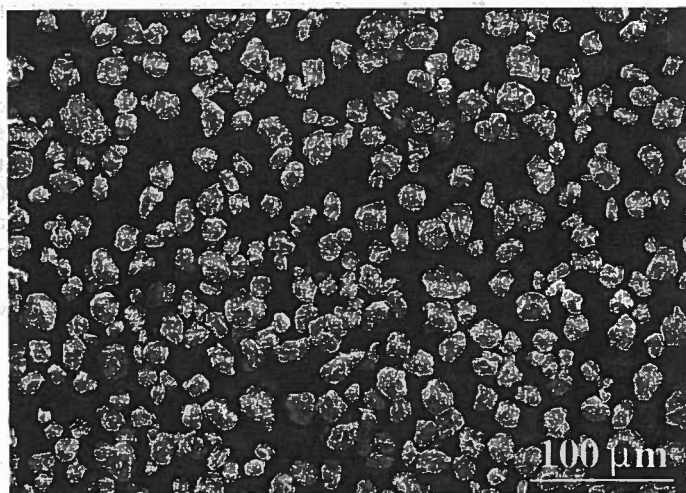


Fig. 1. SEM image of powder particles after 100 h of milling; TiAl45W5 alloy

The single powder particle microstructure revealed by TEM was composed of nanometer sized crystallites embedded in an amorphous matrix. The nanograins formed after only a few hours of milling. Fig 2a. shows the titanium powder particle microstructure of the TiAl5Cr blend after 6 h of milling. The average crystallite diameter measured on an electron micrographs did not exceeded 50 nm. The selected area diffraction patterns were composed of characteristic rings typical for diffraction from polycrystalline sample, however, a superimposed broad "hallo" ring indicates the presence of an amorphous phase (Fig. 2b). The nanostructure results likely from severe plastic deformation applied to particles entrapped between grinding balls during milling and

from instantaneous dynamical recovery of their dense dislocation substructure. Such intense refinement of the particle microstructure is very beneficial for the further powder compaction process since it favors strong reduction in grain size of the consolidated material [9].

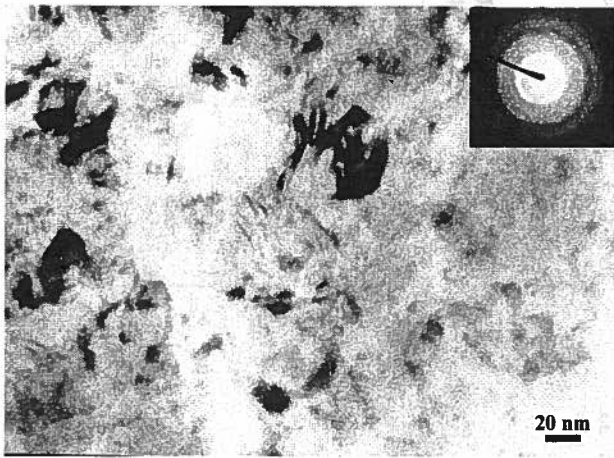


Fig. 2. Bright field TEM microstructure of a powder particle after 6 h of milling and corresponding selected area diffraction pattern

The X-ray diffractograms exhibited clear dependence on the milling time. In general, with the milling time peaks became broader, their intensities decreased and some of them finally vanished. The significant broadening of peaks suggests the formation of an amorphous phase, fine crystalline grains and/or high density of defects. The change in X-ray crystallite size and lattice strain for all alloys occurred in a typical manner, i.e. the crystallite size decreased and lattice strain increased with milling time. The peak positions changed little with milling time, i.e. only slight shift to higher values of 2θ was observed. It indicates a little change in lattice parameter of the processed alloys with milling time. The direction of this shift was expected since atom diameters of dissolved elements in Ti (Al, Cr, V) are smaller than Ti atoms diameter. There are little differences between Ti and Al atom radii (145 vs. 143 pm) and these two elements are basic constituents of all alloys. That is why such a small shift in peak positions occurs on the X-ray diffractograms.

In general, the powder behavior during milling was a typical one for the mechanical alloying process when solid solutions are formed [8]. The exemplary changes in powder physical properties are shown in Table 1. The data in Table 1 pertain to titanium in the TiAl45Cr5 alloy. Fig. 3 shows XRD patterns from as-milled Ti48Al, TiAl45Cr5, TiAl45V5 and TiAl45W5 powders after 100 h of milling. The broad peak at a 2θ position around 45° can be associated to reflections belonging to either pure alloy constituents (such as Al, Ti or TiAl) or the formation of an amorphous phase. Similar ef-

fects were observed by Dutkiewicz et al. in mechanically alloyed TiAl-V alloy [9]. The relatively strong peak at $2\theta = 52^\circ$ comes from chromium. It suggests that Cr dissolves hardly in Ti and forms finally Cr-based solid solution. There is a striking difference between XRD pattern from TiAl5W alloy and those from the other alloys.

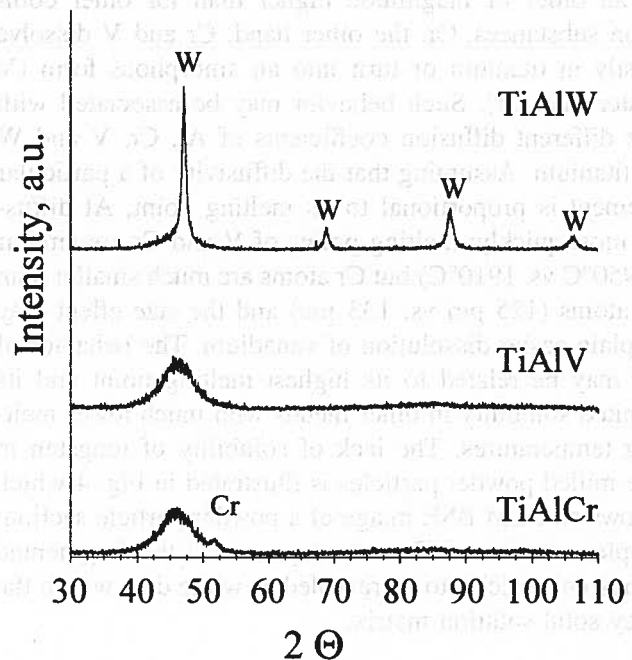


Fig. 3. XRD patterns of milled alloys after 100 h of milling

TABLE 1
Dependence of crystal structure parameters, crystallite size and lattice strain on milling time for titanium in the TiAl45Cr5 powders

Milling time, h	0	6	10	20	50
Cell parameter a = b pm	295.4	295.6	295.5	295.1	293.6
Cell parameter c, pm	468.8	468.8	468.8	468.1	466.7
Ratio c/a	1.587	1.586	1.586	1.586	1.589
Crystallite size, nm	105.2	37.2	35.8	15.3	7.4
Lattice strain, %	0.06	0.16	0.17	1.59	3.33

The crystallite size and lattice strain for W peaks in the TiAl45W5 alloy are shown in Table 2. It is characteristic that lattice strains after 100 h of milling are much smaller than for other alloys after shorter milling times. A visual representation of XRD pattern from the TiAl5W alloy is the same in nature regardless if the alloy was prepared from elemental or prealloyed constituents. The point is that peaks from tungsten remain strong after 100 h of milling though the tungsten content in the alloy is only 5 at. %. This effect arises likely due to the high reference intensity ratio I/I_c for X-ray radiation. The Joint Committee on Powder Diffraction Standards (JCPDS) collect a

file of ratios I/I_c and publish them yearly with the Powder Diffraction File (PDF). In the PDF, I/I_c has been defined as the ratio of the peak height of the strongest line of a sample to the strongest line of hexagonal corundum $\alpha\text{-Al}_2\text{O}_3$ (reflection 113) for 1:1 mixture, by weight, of the two phases. According to Hubbard et al. [10], the reference intensity ratio for tungsten is about 18.0 and is an order of magnitude higher than for other common substances. On the other hand, Cr and V dissolve easily in titanium or turn into an amorphous form (V faster than Cr). Such behavior may be associated with the different diffusion coefficients of Al, Cr, V and W in titanium. Assuming that the diffusivity of a particular element is proportional to its melting point, Al diffuses most quickly; melting points of V and Cr are similar (1950°C vs. 1910°C) but Cr atoms are much smaller than V atoms (125 pm vs. 133 pm) and the size effect may explain easier dissolution of vanadium. The behavior of W may be related to its highest melting point and its limited solubility in other metals with much lower melting temperatures. The lack of solubility of tungsten in the milled powder particles is illustrated in Fig. 4 which shows an SEM BSE image of a powder particle section; implementation of Z contrast permitted the fragmented tungsten particles to be revealed as white dots within the grey solid solution matrix.

TABLE 2

Crystallite size and lattice strain for W peaks in the TiAl45W5 alloy powders

Milling time, h	0	25	30	60	100
Crystallite size, nm	437.6	31.6	29.1	24.0	16.3
Lattice strain, %	0.07	0.40	0.43	0.50	0.70

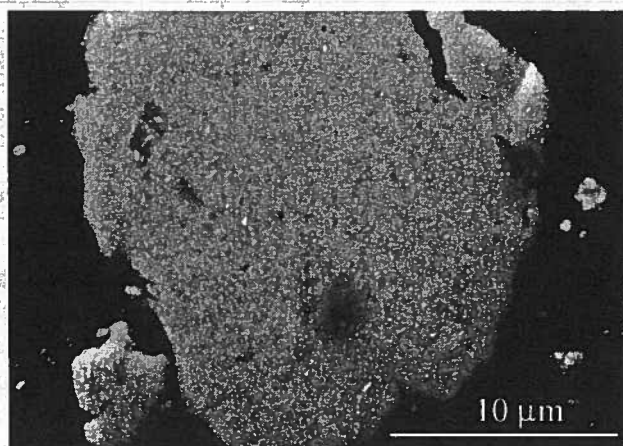


Fig. 4. Typical distribution of tungsten particles (white regions) in a powder particle milled through 100 h; SEM BSE, contrast Z

Annealing of as-milled powder brought about decomposition of solid solutions and amorphous phase into more stable phases. In all alloys only two phases could

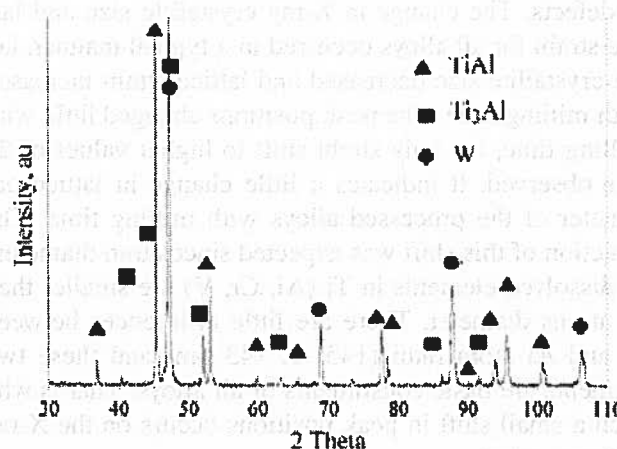
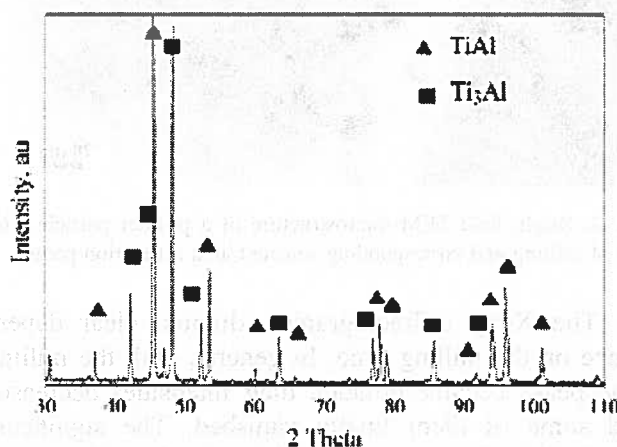
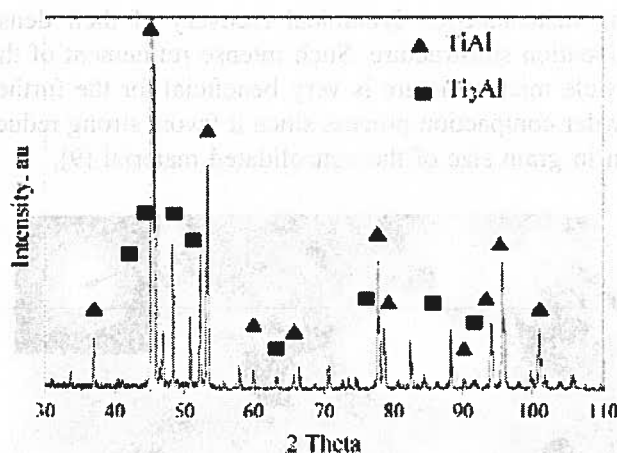


Fig. 5. XRD pattern from powder milled through 100 h and annealed at 1000°C for 5 h; TiAl45W5 alloy

be unequivocally identified by XRD. One of them was the ordered tetragonal $\gamma\text{-TiAl}$ phase and the other was $\alpha_2\text{-Ti}_3\text{Al}$ phase (Fig. 5). On the XRD from TiAl5Cr the $\alpha\text{-Ti}$ -based solid solution as well as an Al_9Cr_4 phase were also detected. The identification of the latter phase was not accurate since peaks coming from this phase exhibited low intensity and their positions were shifted from the theoretical ones. However, the existence of a

Cr-rich phase may be justified since on the XRD from TiAl5Cr powder milled through 100 h the distinct peak in the Cr position was detected (Fig. 3). On the other hand, on the XRD pattern from the TiAl5W alloy well defined peaks from tungsten were detected in addition to the two mentioned phases.

4. Conclusions

The presence of a third element (V, Cr, W) influences the mechanical alloying process of γ -TiAl alloys. The prolong milling of TiAl45V5 alloy leads to its complete amorphisation; the milling of the TiAl45Cr5 alloy in the same conditions leads also to its amorphisation but Cr(Ti, Al) solid solution is also present. Tungsten, on the other hand, do not form solid solutions. Instead, it undergoes heavy refinement during milling and constitute a dispersoid in the consolidated material.

Acknowledgements

The financial support from the Polish Ministry of Education and Science, grant no. 4 T08A 017 25, is greatly appreciated.

REFERENCES

- [1] Y.-W. Kim, D. M. Dimiduk, *Journal of Metals* **43**, 40 (1991).
- [2] Y.-W. Kim, *Journal of Metals* **46**, 30 (1994).
- [3] S. C. Huang, J. C. Chesnutt, *Intermetallic Compounds 2*, ed. J. H. Westbrook, R. L. Fleischer, 73, John Wiley & Sons Inc., 1995.
- [4] F. H. Froes, C. Suryanarayana, in: *Physical Metallurgy and Processing of Intermetallic Compounds*, ed. N. S. Stoloff and V. K. Sikka, 297, Chapman & Hall, 1996.
- [5] C. Choi, Y.-T. Lee, C. S. Lee, *Scripta Mater.* **36**, 821 (1997).
- [6] F. Appel, R. Wagner, *Mat. Sci. Eng.* **R22**, 187 (1998).
- [7] M. A. Morris, M. Leboeuf, *Mat. Sci. Eng.* **A224**, 1 (1997).
- [8] C. Suryanarayana, *Prog. Mater. Sci.* **46**, 1 (2001).
- [9] J. Dutkiewicz, W. Maziarz, *Solid State Phenomena* **101-102**, 117 (2005).
- [10] C. R. Hubbard, E. H. Evans, *J. Appl. Cryst.* **9**, 169 (1976).